International Journal of Heat and Mass Transfer 54 (2011) 2294–2302

Contents lists available at ScienceDirect

International Journal of Heat and Mass Transfer

journal homepage: www.elsevier.com/locate/ijhmt

Resistive heating and electropermeabilization of skin tissue during in vivo electroporation: A coupled nonlinear finite element model

Nataša Pavšelj *, Damijan Miklavčič [1]

Faculty of Electrical Engineering, University of Ljubljana, Tržaška 25, SI-1000 Ljubljana, Slovenia

ARTICLE INFO

Article history:
Available online 4 March 2011

Keywords:
Skin electroporation
Thermal effects
Nonlinear tissue changes
Local transport regions
Numerical modeling

ABSTRACT

The use of electric pulses to increase cell membrane permeability – electroporation – has, among other applications also been used on skin for (a) enhanced transdermal molecular delivery or (b) the delivery of drugs or DNA into viable skin cells. Based on finite element numerical method, we theoretically described skin electropermeabilization and the amount of heating in and around an electrically created pore in the stratum corneum (SC). With the model, we address both, electrical as well as thermal effects on skin tissue, specifically for electrode design and pulse protocols we used for gene electrotransfer in vivo (already published results), where plasmid DNA was injected intradermally with a syringe and external plate electrodes were used for pulse delivery. Theoretical results obtained with the model show no significant further thermal expansion of the aqueous pore for our specific pulse protocol (one short high voltage pulse: 400 V, 100 μs + one longer low voltage pulse: 80 V, 400 ms), as well as no thermal damage to the tissue. With some modifications to the protocol, electroporation could be used to (a) create pores in the SC through which to transport the DNA, and then (b) introduce the DNA into viable skin cells.

1. Introduction

Electroporation or the use of electric pulses to increase cell membrane permeability is present in many molecular biology and medical applications. These include electrochemotherapy, DNA transfection for DNA vaccination and gene therapy, transdermal drug delivery, cell fusion, tissue ablation [1–8]. The concept of reversible electroporation is using electric pulses to establish increased transmembrane voltage on the phospholipid bilayer of a biological cell in order to increase its permeability. This transient permeability increase preserves cell viability and facilitates cell uptake of drugs or DNA. In our published in vivo study [9], a combination of a short high voltage (HV), followed by a longer low voltage (LV) pulse was used to introduce DNA into skin cells. HV pulses alone result in a high level of cell membrane permeabilization (permeabilizing pulse), but very low DNA transfer. However, in combination with one or more LV pulses (electrophoretic pulse), a large increase in DNA transfer occurs [10,11].

Further, electroporation can also be used on skin tissue to permeabilize lipid bilayers of the highly impermeable outermost dead layer of skin – the stratum corneum (SC) – in order to increase transdermal transport of substances such as drugs or other large molecules. Ionic and molecular transport across the skin subjected to high voltage pulses is highly localized in sites termed local transport regions (LTRs) [12–16]. Their size depends on pulse duration, while pulse amplitude dictates their density. Local transport regions are formed as a result of the application of electric pulses on skin and are expanded by resistive heating caused by high local current density due to the electrical conductivity increase inside the LTRs.

During our in vivo experiments, the DNA was introduced into the skin tissue by means of a hypodermic needle. It may, however, be feasible to employ the method of electroporation to first transport molecules through the otherwise impermeable stratum corneum, and second, introduce them into viable skin cells. Yet one of the concerns associated with electrically mediated transdermal delivery and/or gene transfer into viable skin cells is the amount of resistive heating in the tissue. Excessive heating is unwanted not only to avoid skin burns and assure patient safety, but also to avoid damage to viable cells aimed for transfection and to avoid thermally induced damage to the delivered DNA. A lot of work, both theoretical and experimental, has been done to evaluate different pulse parameters and electrode design and their influence on the outcome of the treatment [17]. Although potential excess of the resistive heating during electroporation has been demonstrated [18–22], thermal aspect is mostly overlooked in treatment planning and theoretical analysis of specific applications of electroporation-based treatments.

In this paper, we theoretically describe skin electropermeabilization and study the amount of heating in and around an electrically created pore in the stratum corneum, in order to evaluate

* Corresponding author. Tel.: +386 1 4768 120; fax: +386 1 4264 658.
E-mail addresses: natasa.pavselj@fe.uni-lj.si (N. Pavšelj), damijan.miklavcic@fe.uni-lj.si (D. Miklavčič).
[1] Tel.: +386 1 4768 456; fax: +386 1 4264 658.

0017-9310/$ - see front matter © 2011 Elsevier Ltd. All rights reserved.
doi:10.1016/j.ijheatmasstransfer.2011.02.035

Nomenclature

Abbreviations

SC	stratum corneum
LTR	local transport region
HV	high voltage
LV	low voltage

Physical variables and constants

E	electric field
J	electric current density
V	electric potential
T	temperature
Q_{DC}	resistive heat
σ	electrical conductivity
ρ	mass density
c	specific heat capacity
k	thermal conductivity

possible thermal damage of skin, as well as the delivered DNA. Our theoretical model was based on the finite element method. This method is habitually used in theoretical analysis, efficient protocol, pulse parameters and electrode design and treatment planning [23–26]. Numerical models of electroporation of skin tissue from the aspect of nonlinear changes in tissue electrical conductivity have been described before and proved successful in theoretical explanation of experimentally observed phenomena [27–29]. Specifically on skin, several theoretical models on microscopical or submicroscopical scale were made [30,31]. Further, thermal effects of electric pulses on skin tissue have been studied by Becker and Kuznetsov [32–34]. In our present paper, we address both, electrical as well as thermal effects on skin tissue, specifically for electrode design and pulse protocols used for gene electrotransfer reported previously [9].

2. Theoretical considerations

2.1. Electrical effects on tissue

In [9], unipolar rectangular electric pulses were used for electroporation and gene transfer. The protocols resulting in a successful gene transfection consisted of one short, high-voltage (HV) pulse (amplitude: 280 or 400 V, duration: 100 μs), followed by a long, low voltage (LV) pulse (amplitude: 56 or 80 V, duration: 400 ms). These pulses were much longer than the cell membrane charging time (in the order of a few microseconds), which means that the electric field distribution can be modeled in its steady-state. We used the Laplace steady-state equation, disregarding the transients that occur during the pulse rise time.

$$\nabla \cdot (\sigma \nabla V) = 0 \tag{1}$$

In the above equation, V is the voltage and σ is the conductivity of the material. The electric field in a tissue and electric current passing through the tissue are coexisting and are related by Ohm's law:

$$\mathbf{J} = \sigma \mathbf{E} \tag{2}$$

where **J** is the current density and **E** is the electric field. All of the above equations are linear, however, the electrical behavior of tissue exposed to permeabilizing electric pulses is nonlinear, with the nonlinearity being hidden in tissue material properties. Namely, experiments have shown a nonlinear increase in tissue conductivity due to cell membrane electroporation. In the areas of the tissue where the electric field exceeds a given threshold (termed reversible electroporation threshold), tissue conductivity increases. This phenomenon is termed tissue electropermeabilization. Although both terms are often used as a synonym, in this paper the term *electroporation* is used to describe the method, while *electropermeabilization* is its most important outcome – the increased permeability of the cell membrane.

When referring to its electric properties, skin is highly intricate tissue due to its inhomogeneous structure. Skin epidermis contains different layers, but the one that defines its electric properties the most is the outermost layer, the stratum corneum, composed of dead, flat skin cells. Although very thin (typically around 20 μm), its low electrical conductivity dictates the electric properties of skin. During pulse application, voltage is distributed between skin layers proportionally to their resistivities (as in serially connected resistors – a voltage divider). The electric field in the stratum corneum at the onset of pulse delivery is thus several fold higher than in the dermis and the viable epidermis, where it is well under the electroporation threshold. However, due to nonlinear changes in the tissue, the viable skin layers end up getting exposed to an electric field high enough for a successful tissue electropermeabilization [27–29].

2.2. Heat transfer in tissue

The equation frequently used in the modeling of heat transfer in living tissue is Pennes' bioheat equation [35]. This bioheat model was derived from the measurements of the temperature distribution in the forearm of human subjects and includes the contributions from blood flow and metabolic heat production. However, these contributions were neglected in our model, for several reasons: first, the cooling effect of the blood in the skin during the short electric pulses is very small, compared to the contribution of the resistive heating. Moreover, it has been shown that the application of the electric pulses during electroporation induces fast and significant reduction in blood flow in the treated area [36–38]. And second, the rate of metabolic heat generation during the pulse protocol is, again, negligible compared to the contribution of the resistive heating. Both are especially true in the epidermis (almost no vascularization or metabolic heat production), where most of the heat dissipation takes place during SC electroporation and LTR expansion. Therefore, we used the equation describing heat transfer by conduction in both, electrode, as well as the tissue:

$$\rho \cdot c \frac{\partial T}{\partial t} - \nabla \cdot (k \cdot \nabla T) = Q_{DC} \tag{3}$$

where ρ is the mass density of the material, c is its specific heat capacity, k is its thermal conductivity, T is the temperature and Q_{DC} is resistive heat generated during the pulse(s).

The stratum corneum undergoes several thermally induced phase transitions at elevated temperatures. These temperatures may differ slightly for different animal species, however, in the range of 30–120 °C, roughly four phase transitions were identified: at around 45 °C (lipid packing phase transition), at 70 °C (lipid melting, disappearance of the bilayer structure, increased water permeation), at 85 °C (protein-associated lipid transition, irreversible), and at 100 °C (irreversible protein denaturation) [39–43]. Therefore, it is reasonable to expect changes in thermal properties of skin as the temperature increases during pulse delivery.

Further, a strong coupling between the thermal effects and the conduction current effects exists through the temperature coeffi-

cient for electrical conductivity. Namely, the tissue electrical conductivity increases with temperature, which results in a mutual dependence. However, the temperature coefficient is in the range of 1–3%/°C [44], which is significantly smaller than the increase in tissue conductivity due to electroporation (4-fold for viable skin layers) and was thus neglected.

2.3. The process of LTR formation in skin

It has been shown that molecular and ionic transport across the skin subjected to high voltage pulses is highly localized in transdermal paths termed local transport regions (LTRs) [12–16]. They are formed in the sites of the electrically induced pores through the cell membranes of the stratum corneum (SC) that are expanded into larger LTRs by resistive heating. According to some published studies [12,13], the size of the LTRs depends on pulse duration, while pulse amplitude dictates their density. Specifically for high voltage pulses, the reported size of the resulting LTRs is typically around 100 μm in diameter and their density 25–90 LTRs per 0.1 cm^2. For short pulses, typical minimum LTR size is about 100 μm in diameter; for longer pulses, the sizes increase up to 300 μm. In this paper, the term *pore* is used to refer to an aqueous path through the lipid bilayers of the cells in the SC – the electrical effect of electroporation. On the other hand, the term *local transport region – LTR –* describes a larger aqueous path thermally expanded by resistive heating.

When comparing the conductivity of skin exposed to long pulses with the conductivity of unpulsed skin exposed to temperatures above 70 °C, a similar electrical conductivity is found. Once the pulsing ceases, a fast recovery of the non-heated regions (sites involved in ionic transport) takes place, while only slow recovery occurs at the heated molecular transport sites where the energy dissipation was sufficient to exceed the phase transition temperature of the skin lipids from quasi crystal to liquid crystal state (70 °C).

3. Numerical model

In our previously published work [27], we described the mechanism of the nonlinear process of skin electropermeabilization from the aspect of bulk electrical conductivity changes in tissue, without any regard to the resistive heating in the tissue. In the present paper, we combine both, electrically as well as thermally induced changes in skin tissue during electroporation. The coupled numerical model is based on finite element method and was made in COMSOL Multiphysics. Tissue and electrode setups and pulse parameters were the same as in our previous models [27–29], and are describing our in vivo experiments on rat skin reported previously [9].

3.1. Geometry

Four layers of skin formed into a skin fold were modeled: stratum corneum, viable epidermis, the dermis and the subcutaneous layer of fat and connective tissue. The pulses were delivered through two parallel plate electrodes of 1 mm thickness and 4 mm interelectrode distance. The area of the electrodes in contact with skin was approximately 1 cm × 1 cm. A conductive gel was used in experiments in order to assure good electrical contact between the skin and the electrodes, however, in the numerical model conductive gel was not modeled as a separate layer. By taking advantage of the symmetry in the experimental setup and a repetitive pattern of electrically created pores, only a small part of the geometry was modeled. The whole geometry was thus represented by applying appropriate boundary conditions (see Section 3.2). In this way we reduced the complexity of the model and avoided numerical problems that could render the calculation impossible. The diameter of the SC pore was 15 μm. Although electrically created pores in a biological cell membrane are much smaller (in the order of nm), pathways spanning several layers of flattened corneocytes in the electroporated SC are more likely in the order of μm. Namely, as the diameter of a corneocyte is around 30–50 μm, the pore diameter of 15 μm seems reasonable. The scheme of the skin-electrode experimental setup and the modeled part of a stratum corneum pore with its surroundings are shown in Fig. 1.

3.2. Boundary, initial conditions and material properties

We took advantage of the symmetrical geometry of the skin fold with the electrodes, so only a half of the skin fold was considered

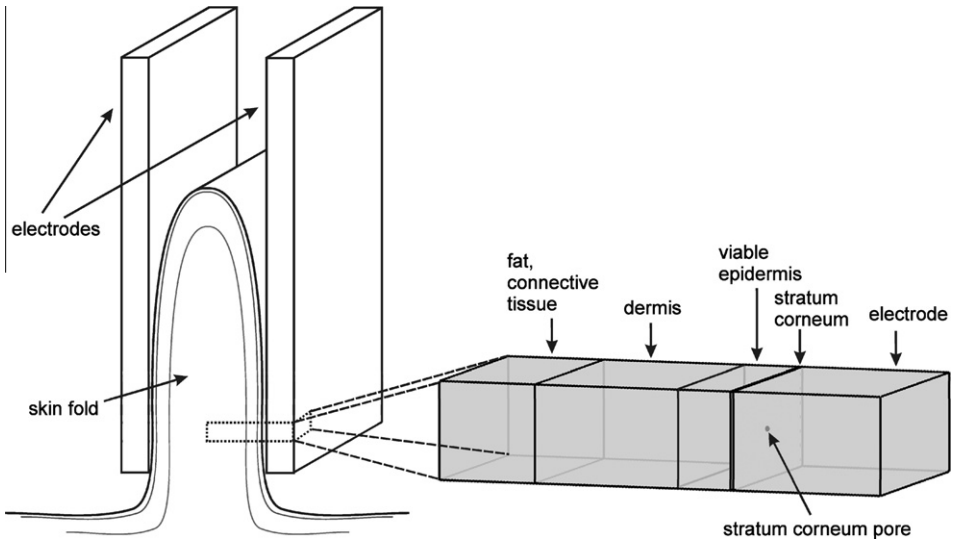

Fig. 1. A schematic picture of the in vivo experimental setup on rat skin and the geometry of the numerical model. The length of this cutout spans the thickness of the skin plus one electrode. The modeled stratum corneum pore with its surroundings represents the repetitive pattern of such pores in the stratum corneum underneath the electrodes. The thicknesses of the modeled layers were: subcutaneous tissue: 650 μm, the dermis: 1000 μm, viable epidermis with papillary dermis: 330 μm, the stratum corneum: 20 μm, the electrode: 1000 μm. The diameter of the pore: 15 μm.

for modeling. This approach can be used when both, the geometry as well as the sources (in our case electric current) exert the same symmetry. Further, even though the distribution of electrically created pores is random, we considered a square lattice arrangement. In this way, we could represent this repetitive pattern with only a small part of the skin underneath the electrode. In our previous models [28,29], a larger pattern of LTR array was modeled and a honeycomb lattice was chosen, as this kind of arrangement is probably closer to the actual LTR distribution than the square lattice. However, when representing an infinite array with a single pore, a square lattice arrangement is easier to model, while still offering a good approximation.

Reported density of local transport regions ranges from 5 to 90 LTRs per 0.1 cm^2 [12–14]. Specifically for high voltage pulses, the density of the resulting LTRs is typically around 25–90 LTRs per 0.1 cm^2 and is increased with increasing pulse voltage. Our model represents the density of 40 pores per 0.1 cm^2.

The boundary conditions were as follows: The pulse voltage amplitude (V_0) was applied to the electrode faces. Because of the symmetry of the skin fold, the electric potential on the tissue bottom face (the midplane of the skin fold) is half of the applied voltage ($V_0/2$). The electrical insulation on tissue side faces (in other words no current flow in the tissue in the direction parallel to the electrodes) represents the infinite pattern of pores. It has to be emphasized that this assumption holds only for the tissue away from the electrode edges. Similarly, there is no heat exchange in the direction parallel to the electrodes (thermal insulation), as well as across the symmetry plane in the middle of the skin fold (thermal insulation on the tissue bottom plane). Further, the electrodes represent a heat sink and the heat is dissipated into surrounding air through the electrode top face. Boundary conditions are compiled in Table 1.

The material properties of tissue before pulse delivery, hence before electrically and thermally induced changes, are based on data reported in the literature. The values of skin layers' electrical conductivity were found in [45–49]. Due to the absence of reported data on electrical conductivity separately for viable epidermis and the dermis, the same conductivity was assigned to both. The same values were used in our previous models [28,29]. The data on thermal properties of skin were found in [32–34,44,50–53]. They were measured mostly on human or pig skin, while our experiments were conducted on rat skin. However, apart from the skin layer thicknesses, the differences are most likely not significant. As the electrodes were made of stainless steel, typical values of electrical and thermal properties for stainless steels were assigned in that domain. The most difficult part was assigning the material properties to the stratum corneum pore. An approximate 150–2500-fold increase of electrical conductivity inside an LTR when compared to SC was reported in [13]. As the applied contact gel fills the newly formed aqueous pore, such increase seems realistic. The electrical conductivity of the pore was thus set to 0.1 (1000-fold increase). Further, no data for thermal properties of the contact gel were found, so in order to set thermal properties of the aqueous pore, the properties of SC were averaged with those of water (water: mass density = 1000 kg/m^3, heat capacity = 4180 J/kg K, thermal conductivity = 0.6 W/mK). Pre-pulse material properties can be found in Table 2.

The initial values of the temperature distribution in the tissue and the electrode were set with the following procedure:

- First the temperature distribution before the tissue-electrode contact was defined. The electrodes and the conductive gel were acclimatized to the ambient temperature in the experimentation room, which was 22 °C. Ambient temperature also decreases the skin temperature by a couple of degrees, compared to body core temperature (37 °C). Therefore, we set the initial temperature of the skin tissue to uniform 34 °C [50].
- Second, we calculated the equilibration temperature after the tissue-electrode contact has been made, and before pulse delivery. The time of equilibration was 30 s.
- This equilibration temperature distribution was used as initial value of the independent variable T during pulse delivery, while the boundary condition on the skin tissue bottom face (the midplane of the skin fold) was set to thermal insulation, due to the symmetrical nature of the setup.

3.3. Meshing and solution procedure

Even though only a small part of the real geometry was modeled, a large number of finite elements could not be avoided. This was due to large dimensional differences between different parts of the model (it includes small structures such as a thin layer of SC and a pore). The stratum corneum with a thermally expanding pore also represent parts with very different material properties, as well as regions of interest, so the mesh in these areas was made denser. The mesh consisted of 68,653 tetrahedral elements and 1,530,199 degrees of freedom.

Table 1
Boundary conditions.

	Electrode top face	Electrode side faces	Tissue side faces	Tissue bottom face
Conductive media DC	$V = V_0$	$V = V_0$	$\mathbf{n} \cdot \mathbf{J} = 0$ (electrical insulation)	$V = V_0/2$
Heat transfer	$\mathbf{n} \cdot (k \cdot T) = h(T_{inf} - T)$ (heat dissipation into surrounding air)	$\mathbf{n} \cdot (k \cdot T) = 0$ (thermal insulation)	$\mathbf{n} \cdot (k \cdot T) = 0$ (thermal insulation)	$n \cdot (k \cdot T) = 0$ (thermal insulation)

V_0 is delivered pulse amplitude.
Heat transfer coefficient, $h = 25$ W/m^2 K.
External temperature, $T_{inf} = 22$ °C (295 K).

Table 2
Pre-pulse material properties.

	SC	SC pore	Viable epidermis	Dermis	Subcut. tissue	Electrodes
Conductive media DC						
El. conductivity, σ (S/m)	0.0001	0.1	0.2	0.2	0.05	$1.35 \cdot 10^6$
Heat transfer						
Mass density, ρ (kg/m^3)	1400	1200	1200	1200	900	7810
Heat capacity, c (J/kg K)	3600	3890	3600	3300	2400	477
Therm. conductivity, k (W/m K)	0.2	0.4	0.24	0.45	0.19	16.9

Table 3
Electro-thermally induced changes of tissue material properties.

	SC	Viable epidermis	Dermis	Subcut. tissue
E-dependent changes[a]				
El. conductivity, σ (S/m)	No change	0.2 → 0.8	0.2 → 0.8	0.05 → 0.2
T-dependent changes				
Mass density, ρ (kg/m^3)	No change	No change	No change	No change
Heat capacity, c (J/kg K)	3600 → 4200[b]	3600 → 4200[b]	No change	No change
Therm. conductivity, k (W/m K)	0.2 → 0.25[c]	0.24 → 0.3[c]	No change	No change
LTR expansion	T > 60 °C: SC → LTR			

[a] (Nonpermeabilized → fully permeabilized tissue).
[b] Linearly in the temperature range from 60 to 85 °C.
[c] Linearly in the temperature range from 37 to 85 °C.

At the beginning of the finite element analysis, the pre-pulse equilibration temperature distribution after the electrode-tissue contact was calculated (see the explanation at the end of previous subsection). After 30 s of equilibration, the pulsing protocol was turned on. During pulse delivery, tissue conductivities in the model were iteratively changed according to the electric field distribution, until the steady state was reached. Tissue permeabilization was gradual between the 600 V/cm and the 1200 V/cm of the local electric field. The current solution was used to look for the areas where the electric field exceeded the pre-set electric field threshold. Tissue conductivity was increased in those areas. This process was described in detail in [27].

Further, various nonlinearities were also included in the thermal part of the model. First, heat capacity and thermal conductivity were dependent on the temperature. We found no reports on temperature dependences of those parameters specifically for skin. However, data could be found for biological tissues in general and specifically for liver tissue and for collagen [54–56]. The reported approximate rise of heat capacity between 60 and 85 °C amounts to 17%, while the rise of thermal conductivity between physiological temperature (37 °C) and 85 °C is about 25%. A significant rise of the temperature is expected in the stratum corneum and the viable epidermis, so temperature dependent parameter changes were assigned only in the outer skin layers. As the effect of temperature on the densities of liquids and solids is small, we assumed no mass density changes. The second thermal nonlinearity was the expansion of the stratum corneum pore when critical temperature was reached. Reported temperature at which lipid melting associated with LTR formation starts is in the temperature range of 60–70 °C [39–43]. The modeled nonlinearities are shown in Table 3.

4. Results and discussion

During our finite element analysis, we used the same pulse protocol as in our published in vivo experiments [9]. The two protocols showing the highest degree of gene electrotransfer were: (a) HV: 400 V, 100 μs + LV: 56 V, 400 ms, and (b) HV: 280 V, 100 μs + LV: 80 V, 400 ms. To get the maximum estimation of the temperature rise, the highest HV and the highest LV of the two protocols was used: HV: 400 V, 100 μs + LV: 80 V, 400 ms. The distribution of temperature in the skin is important to estimate possible damage to viable cells aimed for transfection and to avoid thermally induced damage to the delivered plasmid. With our model, an assessment was made if such protocols cause any significant heating in the stratum corneum that could lead to thermal expansion of the electrically induced pores in the stratum corneum. We also investigated the feasibility to deliver plasmid into the skin transdermally through electro-thermally created pores or local transport regions, instead of an intradermal injection that was used during our in vivo experiments.

Fig. 2 shows the temperature distribution during the high voltage (HV) pulse in and around the electrically created stratum corneum pore (diameter = 15 μm) at 25 μs (a), 50 μs (b), 75 μs (c) and 100 μs (d). It is evident from the figure that no significant thermally induced expansion of the pore (temperatures above 60 °C) takes place during the HV pulse. Maximum reached temperatures inside the pore were: at 25 μs: 65 °C, at 50 μs: 100 °C, at 75 μs: 133 °C and at 100 μs: 161 °C. These peak temperatures, although quite high make no direct damage to the tissue, as they are reached inside a pore that is filled with contact gel. The produced heat does, however, get dissipated into the neighboring domains – the SC and the viable epidermis. Still, in the viable epidermis, the temperature rise is spatially limited to the area just below the stratum corneum. The threshold temperature causing skin burns is 45 °C, however, the duration of exposure needs to be much longer (1 h) in order to cause skin burns at this temperature. About 1 s of exposure is needed at 70 °C. The time of exposure of epidermis to temperatures above 70 °C in our case was shorter (the whole pulse protocol is less than half a second), so we can safely conclude that no significant damage of viable tissue was caused. Indeed, during our published in vivo experiments [9], using the described experimental setup and protocols, a tolerance study was also done and the results showed no burns or erythema. Moreover, the histological study of the treated skin was performed and it showed no damage in the structure of the skin. Some short-term redness was observed with the naked eye a few minutes after pulsing. It was consistently lower on the anode side of the treated area (when compared to the cathode side), which shows that this transient redness can be attributed to local changes in ion concentration or pH imbalance, and is not a consequence of temperature increase. This in vivo finding is further confirmed with the presented theoretical results.

The electrically and thermally induced changes of tissue material properties at the end of HV pulse are shown in Fig. 3. Dark color in the stratum corneum around the LTR shows the areas heated above 60 °C (threshold for thermally induced LTR expansion). Shades of gray in the viable epidermis denote part of the tissue of increased cell membrane permeability, that is the areas where the electric field reversible electroporation threshold is reached. Tissue permeabilization is gradual, from 600 V/cm (light gray) to 1200 V/cm (dark gray, fully permeabilized tissue). In terms of tissue conductivity, white color denotes the prepulse value of 0.2 S/m, while the dark gray color represents fully permeabilized tissue (0.8 S/m).

Fig. 4 shows the temperature distribution during the low voltage (LV) pulse in and around the stratum corneum pore at 100 μs (a), 1 ms (b), 6 ms (c) and 400 ms (d) of the LV pulse. The results reveal that the amount of resistive heating for the duration of the 400 ms of LV pulse is lower than the amount of heat dissipation deeper into the skin. No further thermally induced expansion of the highly conductive stratum corneum pore takes place during the LV pulse. Maximum reached temperatures inside the pore were: at 100 μs: 126 °C, at 1 ms: 64 °C, at 6 ms: 58.6 °C and at

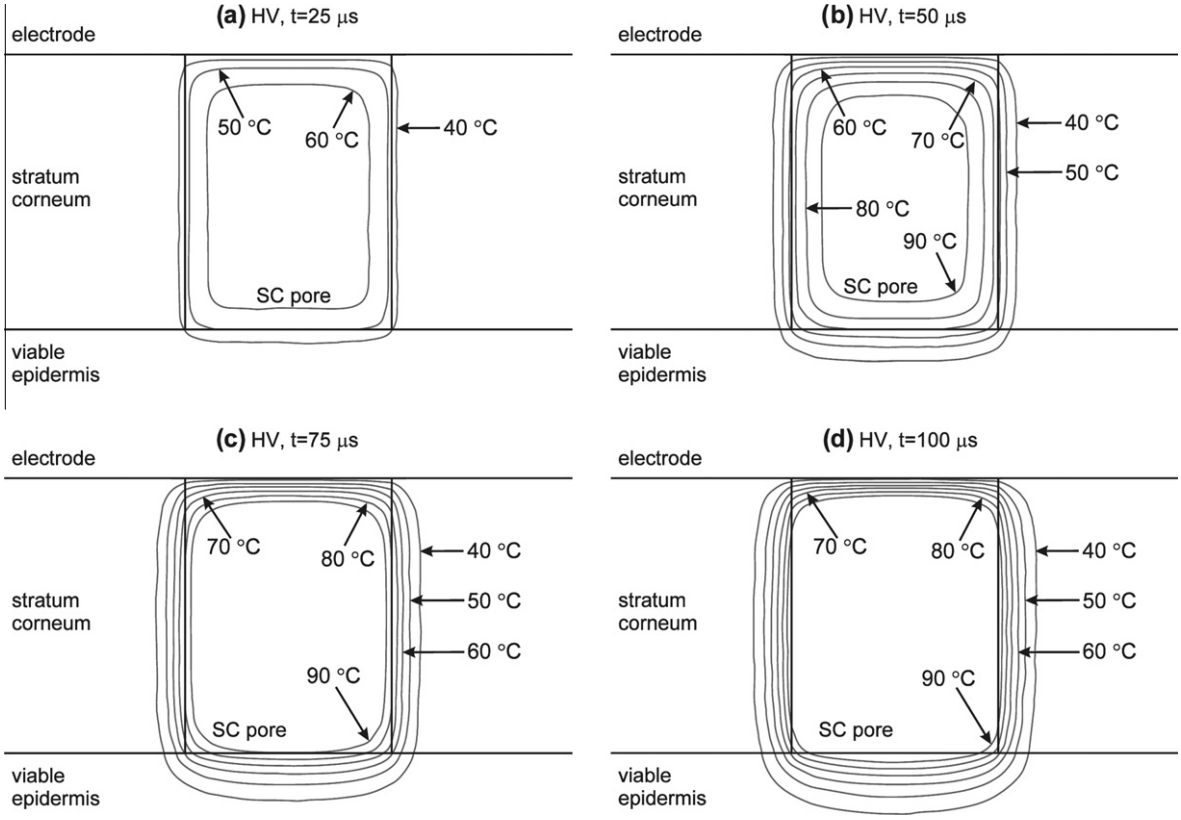

Fig. 2. Isotherms during the high voltage (HV) pulse in and around the electrically created stratum corneum pore (diameter = 15 μm). Pulse duration was 100 μs, pulse amplitude was 400 V. Temperature distribution is shown at 25 μs (a), 50 μs (b), 75 μs (c) and 100 μs (d) in the section plane cut through the middle of the SC pore, perpendicularly to skin surface.

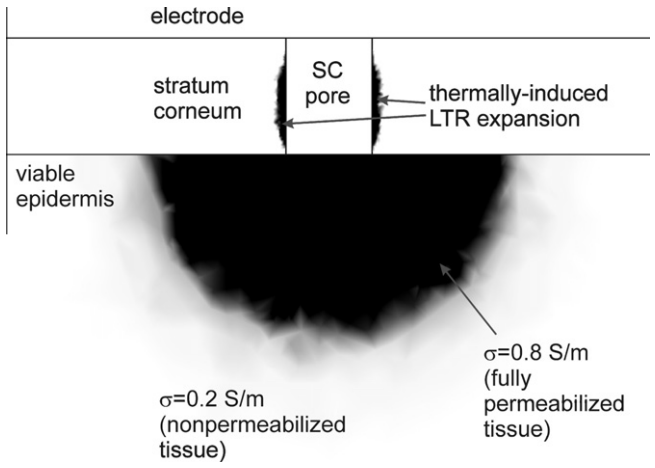

Fig. 3. Electrically and thermally induced changes of tissue material properties at the end of the HV pulse. Dark color in the stratum corneum around the SC pore: thermally induced LTR expansion. Dark gray in the viable epidermis: electropermeabilized tissue.

400 ms: 60.5 °C. The maximum temperature inside the pore is dropping sharply for the first 6 ms of the LV pulse (minimum temperature is 58.6 °C), then slightly increasing for the rest of the pulse, reaching 60.5 °C at the end.

It is evident from the results that no significant thermal expansion of the electrically-created aqueous pore in the stratum corneum takes place during either the HV or the LV pulse. Further, no significant damage of viable tissue underneath the stratum corneum (the epidermis) was caused as a result of resistive heat dissipation. Although comparing the results of our model with other published theoretical analyses of skin electroporation is difficult due to different geometrical and pulse parameters, some parallels can nevertheless be drawn. In Becker's papers [32,34], similar geometry of the skin fold with the plate electrodes was used. The delivered square pulses were in the range of the pulse amplitude used during our HV pulse (300 of 275 V). However, the pulses were much longer (250 ms), which led to a significant heating and LTR creation. Nevertheless, Becker's results at 10 or 20 ms of the applied pulse (still 100 or 200 times longer than our 100 μs HV) show that the temperature rise around the SC pore is still limited to the direct vicinity of the 15 μm pore. Similarly, limited temperature rise inside a 50 μm pore during single exponentially decaying pulse (time constant: 1 or 10 ms, 70 V amplitude across SC alone) was also demonstrated in a theoretical model by Martin et al. [30].

A number of in vitro experimental studies were done on skin studying the formation of aqueous pores through the SC as a result of electroporation [12–14]. The main question was whether the increase in the SC permeability is fundamentally an electrical or a thermal phenomenon. A widely accepted answer is that while the electroporation of cell membranes is responsible for the creation of small pores in the SC, the thermal effect causes their expansion and the formation of the larger local transport regions (LTRs). Unfortunately, the described in vivo setup is hard to compare to different in vitro experimental circumstances where usually thin specimens of SC with some epidermal tissue placed in a permeation chamber were used. However, it seems that bigger amount of electrical energy needs to be delivered than during our HV + LV protocol in order to observe larger local transport regions through the SC. Namely, a number of exponentially decaying electroporation pulses of time constant at least 1 ms or longer (up to 300 ms) were usually used in vitro. In contrast, our electroporative

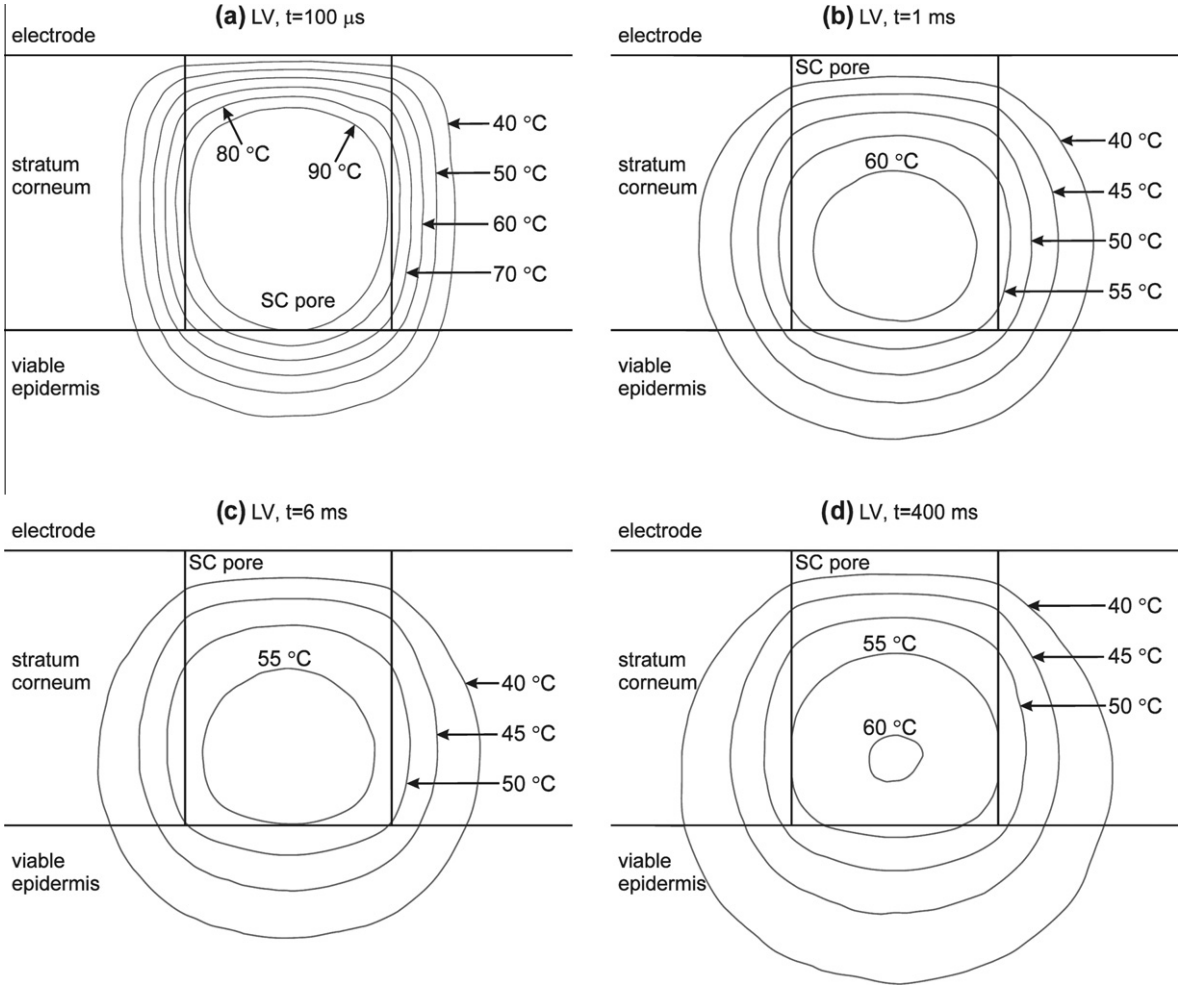

Fig. 4. Isotherms during the low voltage (LV) pulse in and around the electrically created stratum corneum pore (diameter = 15 μm). Pulse duration was 400 ms, pulse amplitude was 80 V. Temperature distribution is shown at 100 μs (a), 1 ms (b), 6 ms (c) and 400 ms (d) in the section plane cut through the middle of the pore, perpendicularly to skin surface.

high voltage pulse was too short, while the amplitude of the following, albeit longer electrophoretic pulse was too low to cause any significant heating and LTR expansion. We also confirmed this in vitro on a dermatomed skin in a permeation chamber. No local transport regions were observed using our described HV + LV pulse protocol (data not published).

Although our model shows that no large LTRs are produced as a result of the pulse protocol used, one more aspect of a electro-thermal synergistic effect of electric pulses on skin, not included in our model, needs to be pointed out. Namely, transdermal voltage causing SC electroporation is temperature dependent; in other words, the probability of further electroporation is increased in the heated regions [21]. Consequently, resistive heating in the vicinity of the electrically created pore will lead to more pore formation and thus larger area involved in transdermal transport. Further, with the periodic boundary conditions in the model we represented the density of 40 pores per 0.1 cm^2, which is the reported LTR density for high voltage pulses [12–14]. Most likely, more pores in the SC are created due to cell membrane electroporation, however, only a portion of them are expanded into LTRs under favorable pulse conditions.

Due to the electrical breakdown and the increased permeability of the stratum corneum, the viable cells end up getting exposed to an electric field high enough to cause cell membrane permeabilization, which is crucial for successful gene transfection. As shown by the model, the permeabilized area extends beyond the dimensions of the pore in the SC (Fig. 3), which yields enough viable cells for gene transfection. Further, as already mentioned, it is likely that the number of such pores is much higher than the modeled 40 pores per 0.1 cm^2, making the volume of permeabilized cells in the viable layers even larger.

With respect to the potential damage to the plasmid during our in vivo experiments we can safely conclude that no thermally induced harm was done. Namely, the plasmid was injected intradermally with a syringe into viable skin layers where thermal dissipation is low. However, we also wanted to explore the feasibility of using electroporation as a two-stage process for gene delivery in skin: (a) to create pores in the SC through which to transport the DNA, then (b) introduce the DNA into viable skin cells. The biggest obstacle is the amount of resistive heat produced during the pulse protocol. Although no significant damage is done to the tissue, the temperature in the transdermal paths in the SC is high and could damage the plasmid. However, with a modification of the pulsing protocol, the two-stage process of gene delivery is still feasible. Firstly, one or more HV pulses could be used to permeabilize the SC and create aqueous pores. After that, a few seconds without pulsing should elapse in order to allow heat dissipation and lower the peak temperatures inside the pores. Secondly, plasmid DNA should be applied topically on the skin and either left to diffuse or be delivered electrophoretically through the SC. Namely, according to the literature [12,13], once the pulsing ceases, only slow SC recovery (no pore resealing) occurs at

the sites where the temperature has exceeded 70 °C. As the final stage of the protocol, an HV + LV pulse protocol could be used in order to achieve gene transfection of viable skin cells. An advantage of this method is the large volume of permeabilized viable epidermal cells in the direct vicinity of the aqueous transdermal delivery paths (see Fig. 3), which increases the odds of a high level electrotransfer.

5. Conclusions

In this paper, we theoretically describe skin electropermeabilization addressing both, electrical as well as thermal effects on skin tissue. The electrode design and pulse protocols we describe were used for gene electrotransfer in vivo, where plasmid DNA was injected intradermally with a syringe and square electric pulses were delivered to the skin tissue with external plate electrodes. We analyzed the amount of heating in and around an electrically created pore in the stratum corneum, to evaluate possible thermal damage of skin, as well as the delivered DNA. Further, we investigated the feasibility to use electroporation as a two-stage process for gene delivery in skin: (a) to deliver plasmid DNA into the skin transdermally through electro-thermally created aqueous paths in the SC, instead of an intradermal injection, then (b) achieve successful DNA electrotransfer into viable skin cells. The results of our theoretical model demonstrate that no significant further thermal expansion of the electrically-created pores in the SC takes place during the pulse delivery. Furthermore, no significant damage to the viable skin was caused as a result of resistive heat dissipation. This finding was also confirmed during the experimental tolerance study in vivo, published in [9]. Also, with some modifications to the used HV + LV protocol, electroporation of skin could potentially be used as a successful two-stage process of gene delivery.

Theoretical evaluation of different pulse parameters and tissue-electrode geometrical setups is becoming commonplace in electroporation-based treatments, however, thermal aspect is mostly overlooked. Since the amount of resistive heat is different for every specific application, thermal effects should be considered in such theoretical models, as merely a general estimation is often not sufficient.

Acknowledgments

This work was funded by the Slovenian Research Agency.

References

[1] G. Sersa, D. Miklavcic, M. Cemazar, Z. Rudolf, G. Pucihar, M. Snoj, Electrochemotherapy in treatment of tumours, EJSO 34 (2008) 232–240.
[2] L. Mir, Nucleic acids electrotransfer-based gene therapy (electrogenetherapy): past, current, and future, Mol. Biotechnol. 43 (2009) 167–176.
[3] J. Escoffre, T. Portet, L. Wasungu, J. Teissie, D. Dean, M. Rols, What is (still not) known of the mechanism by which electroporation mediates gene transfer and expression in cells and tissues, Mol. Biotechnol. 41 (2009) 286–295.
[4] J. Escobar-Chavez, D. Bonilla-Martinez, M. Villegas-Gonzalez, A. Revilla-Vazquez, Electroporation as an efficient physical enhancer for skin drug delivery, J. Clin. Pharmacol. 49 (2009) 1262–1283.
[5] R. Davalos, L. Mir, B. Rubinsky, Tissue ablation with irreversible electroporation, Annal. Biomed. Eng. 33 (2005) 223–231.
[6] C. Ramos, J. Teissie, Electrofusion: a biophysical modification of cell membrane and a mechanism in exocytosis, Biochimie 82 (2000) 511–518.
[7] D. Hannaman, Electroporation for DNA immunization: clinical application, Exp. Rev. Vaccines 9 (2010) 503–517.
[8] A. Gothelf, J. Eriksen, P. Hojman, J. Gehl, Duration and level of transgene expression after gene electrotransfer to skin in mice, Gene Therapy (2010).
[9] N. Pavselj, V. Preat, DNA electrotransfer into the skin using a combination of one high- and one low-voltage pulse, J. Control. Release 106 (2005) 407–415.
[10] S. Satkauskas, M. Bureau, M. Puc, A. Mahfoudi, D. Scherman, D. Miklavcic, et al., Mechanisms of in vitro DNA electrotransfer: respective contributions of cell electropermeabilization and DNA electrophoresis, Mol. Therapy 5 (2002) 133–140.
[11] M. Kanduser, D. Miklavcic, M. Pavlin, Mechanisms involved in gene electrotransfer using high-and low-voltage pulses – an in vitro study, Bioelectrochemistry 74 (2009) 265–271.
[12] U.F. Pliquett, R. Vanbever, V. Preat, J.C. Weaver, Local transport regions (LTRs) in human stratum corneum due to long and short 'high voltage' pulses, Bioelectrochem. Bioenerg. 47 (1998) 151–161.
[13] U. Pliquett, C. Gusbeth, Surface area involved in transdermal transport of charged species due to skin electroporation, Bioelectrochemistry 65 (2004) 27–32.
[14] R. Vanbever, U.F. Pliquett, V. Preat, J.C. Weaver, Comparison of the effects of short, high-voltage and long, medium-voltage pulses on skin electrical and transport properties, J. Control. Release 69 (1999) 35–47.
[15] J.C. Weaver, T.E. Vaughan, Y.A. Chizmadzhev, Theory of electrical creation of aqueous pathways across skin transport barriers, Adv. Drug Delivery Rev. 35 (1999) 21–39.
[16] U. Pliquett, Mechanistic studies of molecular transdermal transport due to skin electroporation, Adv. Drug Delivery Rev. 35 (1999) 41–60.
[17] A. Gothelf, J. Gehl, Gene electrotransfer to skin; review of existing literature and clinical perspectives, Curr. Gene Therapy 10 (2010) 287–299.
[18] R.V. Davalos, B. Rubinsky, L.M. Mir, Theoretical analysis of the thermal effects during in vivo tissue electroporation, Bioelectrochemistry 61 (2003) 99–107.
[19] R.V. Davalos, B. Rubinsky, Temperature considerations during irreversible electroporation, Int. J. Heat Mass Transfer 51 (2008) 5617–5622.
[20] I. Lacković, R. Magjarević, Three-dimensional finite-element analysis of Joule heating in electrochemotherapy and in vivo gene electrotransfer, IEEE Trans. Dielectr. Electr. Insul. 16 (2009) 1339.
[21] U. Pliquett, Joule heating during solid tissue electroporation, Med. Biol. Eng. Comput. 41 (2003) 215–219.
[22] C. Daniels, B. Rubinsky, Electrical field and temperature model of nonthermal irreversible electroporation in heterogeneous tissues, J. Biomech. Eng. 131 (2009) 071006.
[23] N. Pavselj, D. Miklavcic, Numerical modeling in electroporation-based biomedical applications, Radiol. Oncol. 42 (2008) 159–168.
[24] D. Miklavcic, S. Corovic, G. Pucihar, N. Pavselj, Importance of tumour coverage by sufficiently high local electric field for effective electrochemotherapy, EJC Suppl. 4 (2006) 45–51.
[25] A. Zupanic, S. Corovic, D. Miklavcic, Optimization of electrode position and electric pulse amplitude in electrochemotherapy, Radiol. Oncol. 42 (2008) 93–101.
[26] D. Miklavcic, M. Snoj, A. Zupanic, B. Kos, M. Cemazar, M. Kropivnik, et al., Towards treatment planning and treatment of deep-seated solid tumors by electrochemotherapy, Biomed. Eng. 9 (2010).
[27] N. Pavselj, V. Preat, D. Miklavcic, A numerical model of skin electropermeabilization based on in vivo experiments, Annal. Biomed. Eng. 35 (2007) 2138–2144.
[28] N. Pavselj, D. Miklavcic, Numerical models of skin electropermeabilization taking into account conductivity changes and the presence of local transport regions, IEEE Trans. Plasma Sci. 36 (2008) 1650–1658.
[29] N. Pavselj, D. Miklavcic, A numerical model of permeabilized skin with local transport regions, IEEE Trans. Biomed. Eng. 55 (2008) 1927–1930.
[30] G.T. Martin, U.F. Pliquett, J.C. Weaver, Theoretical analysis of localized heating in human skin subjected to high voltage pulses, Bioelectrochemistry 57 (2002) 55–64.
[31] U. Pliquett, C. Gusbeth, R. Nuccitelli, A propagating heat wave model of skin electroporation, J. Theor. Biol. 251 (2008) 195–201.
[32] S.M. Becker, A.V. Kunetsov, Local temperature rises influence in vivo electroporation pore development: a numerical stratum corneum lipid phase transition model, J. Biomech. Eng. – Trans. ASME 129 (2007) 712–721.
[33] S.M. Becker, A.V. Kuznetsov, Thermal damage reduction associated with in vivo skin electroporation: a numerical investigation justifying aggressive pre-cooling, Int. J. Heat Mass Transfer 50 (2007) 105–116.
[34] S.M. Becker, A.V. Kuznetsov, Thermal in vivo skin electroporation pore development and charged macromolecule transdermal delivery: a numerical study of the influence of chemically enhanced lower lipid phase transition temperatures, Int. J. Heat Mass Transfer 51 (2008) 2060–2074.
[35] H.H. Pennes, Analysis of tissue and arterial blood temperatures in the resting human forearm, J. Appl. Physiol. 1 (1948) 93.
[36] G. Sersa, T. Jarm, T. Kotnik, A. Coer, M. Podkrajsek, M. Sentjurc, et al., Vascular disrupting action of electroporation and electrochemotherapy with bleomycin in murine sarcoma, Brit. J. Cancer 98 (2008) 388–398.
[37] G. Sersa, M. Cemazar, C.S. Parkins, D.J. Chaplin, Tumour blood flow changes induced by application of electric pulses, Eur. J. Cancer 35 (1999) 672–677.
[38] T. Jarm, M. Cemazar, D. Miklavcic, G. Sersa, Antivascular effects of electrochemotherapy: implications in treatment of bleeding metastases, Exp. Rev. Anticancer Therapy 10 (2010) 729–746.
[39] G. Golden, D. Guzek, A. Kennedy, J. Mckie, R. Potts, Stratum–Corneum lipid phase-transitions and water barrier properties, Biochemistry 26 (1987) 2382–2388.
[40] S.M. Al-Saidan, B.W. Barry, A.C. Williams, Differential scanning calorimetry of human and animal stratum corneum membranes, Int. J. Pharmaceutics 168 (1998) 17–22.
[41] H. Tanojo, J.A. Bouwstra, H.E. Junginger, H.E. Boddé, Thermal analysis studies on human skin and skin barrier modulation by fatty acids and propylene glycol, J. Therm. Anal. Calorim. 57 (1999) 313–322.
[42] C. Silva, S. Nunes, M. Eusébio, A. Pais, J. Sousa, Thermal behaviour of human stratum corneum, Skin Pharmacol. Physiol. 19 (2006) 132–139.

[43] C.L. Silva, S.C.C. Nunes, M.E.S. Eusébio, J.J.S. Sousa, A. Pais, Study of human stratum corneum and extracted lipids by thermomicroscopy and DSC, Chem. Phys. Lipids 140 (2006) 36–47.
[44] F.A. Duck, Physical Properties of Tissue: A Comprehensive Reference Book, Academic Press, London, 1990.
[45] C. Gabriel, S. Gabriel, E. Corthout, The dielectric properties of biological tissues: I. Literature survey, Phys. Med. Biol. 41 (1996) 2231–2249.
[46] S. Gabriel, R.W. Lau, C. Gabriel, The dielectric properties of biological tissues: II. measurements in the frequency range 10 Hz to 20 GHz, Phys. Med. Biol. 41 (2004) 2251–2269.
[47] U. Pliquett, R. Langer, J.C. Weaver, Changes in the passive electrical properties of human stratum corneum due to electroporation, Biochim. Biophys. Acta 1239 (1995) 111–121.
[48] T. Yamamoto, Y. Yamamoto, Dielectric constant and resistivity of epidermal stratum corenum, Med. Biol. Eng. 14 (1976) 494–499.
[49] T. Yamamoto, Y. Yamamoto, Electrical properties of the epidermal stratum corneum, Med. Biol. Eng. 14 (1976) 151–158.
[50] T.R. Gowrishankar, D.A. Stewart, G.T. Martin, J.C. Weaver, Transport lattice models of heat transport in skin with spatially heterogeneous, temperature-dependent perfusion, BioMed. Eng. 3 (2004) 42.
[51] S.A. Bellia, A. Saidane, M. Benzohra, J.M. Saiter, A. Hamou, Dimensional soft tissue thermal injury analysis using transmission line matrix (TLM) method, Int. J. Numer. Model. 21 (2008) 531–549.
[52] S. Aliouat Bellia, A. Saidane, A. Hamou, M. Benzohra, J.M. Saiter, Transmission line matrix modelling of thermal injuries to skin, Burns 34 (2008) 688–697.
[53] M. Gasperin, Š. Juricic, The uncertainty in burn prediction as a result of variable skin parameters: an experimental evaluation of burn-protective outfits, Burns 35 (2009) 970–982.
[54] D. Haemmerich, I. Santos, D.J. Schutt, J.G. Webster, D.M. Mahvi, In vitro measurements of temperature-dependent specific heat of liver tissue, Med. Eng. Phys. 28 (2006) 194–197.
[55] D. Haemmerich, D.J. Schutt, I. Santos, J.G. Webster, D.M. Mahvi, Measurement of temperature-dependent specific heat of biological tissues, Physiol. Measur. 26 (2005) 59–67.
[56] A. Bhattacharya, R.L. Mahajan, Temperature dependence of thermal conductivity of biological tissues, Physiol. Measur. 24 (2003) 769–783.